The synergies between displacement damage creation and hydrogen presence: the effect of D ion energy and flux

Sabina Markelj[1], Matic Pečovnik[1], Thomas Schwarz-Selinger[2] and Mitja Kelemen[1,3]

[1] Jožef Stefan Institute, Ljubljana, Slovenia
[2] Max-Planck-Institut für Plasmaphysik, Garching, Germany
[3] Jožef Stefan International Postgraduate School, Ljubljana, Slovenia

E-mail: sabina.markelj@ijs.si

The content of this manuscript is identical to
S. Markelj et al, Phys. Scr. 97 (2022) 024006 ; https://doi.org/10.1088/1402-4896/ac4860

Received 15 September 2021 / Accepted for publication 22.December 2021 / Published 24 January 2022

Abstract

In this work the synergism between displacement damage creation and presence of hydrogen isotopes was studied. Tungsten samples were irradiated by 10.8 MeV W ions with or without the presence of D ions with two different energies of 300 eV/D and 1000 eV/D and different temperatures. In order to compare the results obtained with different exposure parameters the samples were afterwards additionally exposed to D ions at 450 K to populate the created defects. By increasing the W irradiation time, ion flux and energy, the increase of D concentration and D retention was observed as measured by nuclear reaction analysis and thermal desorption spectroscopy. By fitting the D depth profiles and D desorption spectra by the rate equation code MHIMS-R we could see that additional fill-levels were populated with higher flux and ion energy which ends up in higher final D concentration and retention as compared to experiments with lower D flux and energy.

Keywords: tungsten, displacement damage, defect stabilization, hydrogen isotopes, deuterium

1. Introduction

In future thermonuclear devices such as DEMO displacement damage by 14 MeV fusion neutrons will be created in the plasma-facing materials while they are exposed to high fluxes of ions and neutrals of hydrogen isotopes (HIs) at elevated temperatures. For this reason, the synergism between displacement damage creation and presence of HIs needs to be studied for predicting fuel retention and transport in future fusion devices [1, 2]. Tungsten (W) and tungsten-based alloys were identified as prime candidates as plasma facing material [1, 3] due to low HI retention in tungsten, low sputtering yield and good thermal conductivity.

In order to be able to describe the interaction between HI and defects in tungsten lattice as well as the creation and evolution of defects and their dependence on temperature and HI flux one needs to isolate and understand the individual processes [4]. In recent years particle beam experiments were performed to address individual aspects. To study creation and evolution of defects with temperature, recrystallized polycrystalline W samples were first irradiated by 20 MeV or 10.8 MeV W ions and then sequentially exposed to low-energy deuterium (D) to populate the defects [5, 6, 7]. D retention and desorption kinetics were obtained by measuring D depth profiles and D thermal desorption spectra, showing that created defects act as traps for D and the defect densities decrease with temperature. To study the synergism between defects and HI, W samples were simultaneously irradiated by

10.8 MeV W ions and exposed to low-energy D at different temperatures ranging from 450 K to 1100 K [6, 7]. After the simultaneous W/D exposure the samples were additionally exposed to D in order to populate all the defects created beforehand. An increase in maximum D concentration was observed as compared with the sequential exposures by a factor of two for low temperatures decreasing for higher temperatures. In order to explain the observed results the macroscopic rate equation modelling code MHIMS [8, 9] was used and further developed [10]. In order to interpret the effect of the D presence during the creation of displacement damage a new rate equation model was included that couples a displacement damage creation model with the kinetics of D transport and trapping [10]. The model enabled us to explain the change in D concentration by the trapped amount of D during the simultaneous exposures. The increase of the defect density due to the presence of D was parametrized by a stabilization factor and the number of defects populated by D [10]. This is in line with theoretical calculations predicting that trapped D in a vacancy prevents vacancy annihilation with self-interstitials [11] and, therefore, stabilizes the defect.

In this work we wanted to expand the previous studies and explore how different exposures/irradiation times and higher D ion fluxes and lower exposure temperatures influence defect creation when hydrogen isotopes are present.

2. Experiment

For the experiment Plansee 12×15 mm^2 and 0.8 mm thick hot-rolled recrystalized polycrystalline tungsten samples with a purity of 99.997 wt. % were used. They were prepared in the same way as described in detail in [6].

Experiments were conducted in the INSIBA chamber in a configuration which can be seen in figure 1. The D ion beam was produced by a commercial electron cyclotron resonance (ECR) ion gun (Tectra Gen II www.tectra.de/sputter.html, energy range 0.025-5 keV). The optimal working conditions and characteristics of the ion gun were determined and described in detail in Ref. [6]. A collimator was placed in front of the ion gun exit orifice in order to limit the beam only to the sample surface and thus not irradiate the surrounding objects. The ion gun was positioned at an angle of 51° with respect to the MeV ion beam. The ECR gun was mounted on a linear translator. This allowed us to move the ion gun closer or further away from the sample surface and therefore vary the D ion flux. At the closest position the distance between the D ion exit orifice and the W sample surface is approximately 33 mm. With the D ion gun so close to the sample we ensured the D ion flux to be more homogeneous across the sample surface, as compared to the previous set-up with a focussing Einzel lens [6]. The D ion current was measured during the D ion exposure on the sample. The distribution of the D flux was additionally measured using a Faraday cup with a 2 mm diameter circular orifice as described in detail in [12]. In this work we have used two acceleration voltages for D ion exposure. The acceleration voltage of the D ion gun was either 1 kV or 3.1 keV while the sample was biased with a voltage of a +100 V. As the majority of the D ions coming from the ion gun are in the form of D_3^+ ions, the energy of the impacting D ions is approximately 300 eV/D or 1000 eV/D, respectively. The beam shape of D ions changes with the acceleration voltage. We have obtained a rather homogeneous distribution of the D ion flux within the sample dimensions for 1 kV acceleration voltage and more a peaked distribution for the 3.1 keV case. Typical ion current on the sample for 300 eV/D beam was 10±2 μA and for 1 keV/D beam was 17±3 μA. With the current measurement and the measurement of the beam profile by eroding an amorphous hydrogenated carbon thin film [13, 6] or by a Faraday cup [12] we estimated the D ion flux at the center of the beam profile to be (4±1)×10^{18} D/m^{2}s for 300 eV/D and (8±1.5)×10^{18} D/m^{2}s for 1000 eV/D. By using two different energies of D ions, the implantation depth and concentration of mobile D in the sample is varied.

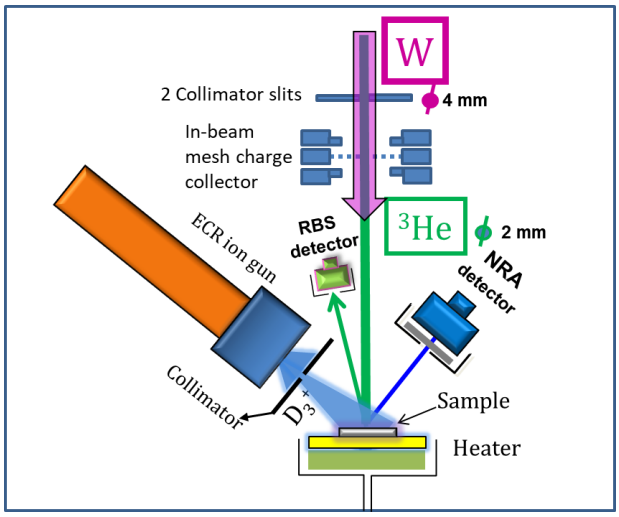

Figure 1: Configuration of the INSIBA setup for the present experiments showing the heated holder together with the low energy ECR ion gun for D exposure together with the MeV W ion beam for damage creation and the detectors and beam arrangement for the NRA and RBS analysis.

In order to create displacement damage in W samples 10.8 MeV W ions were created by a 2 MV tandetron accelerator. The W ion irradiation was performed either with or without D ion exposure, the so-called simultaneous or sequential experiment, respectively, as explained in detail in [6]. The annotation for simultaneous W and D ion irradiation is "W/D". After this the samples were additionally exposed to D ions at low temperature of 450 K in order to populate the whole damage range by D and is denoted as "W/D-D". In the sequential case the samples were first irradiated by W ions only and then later exposed to D ions at 450 K to populate all

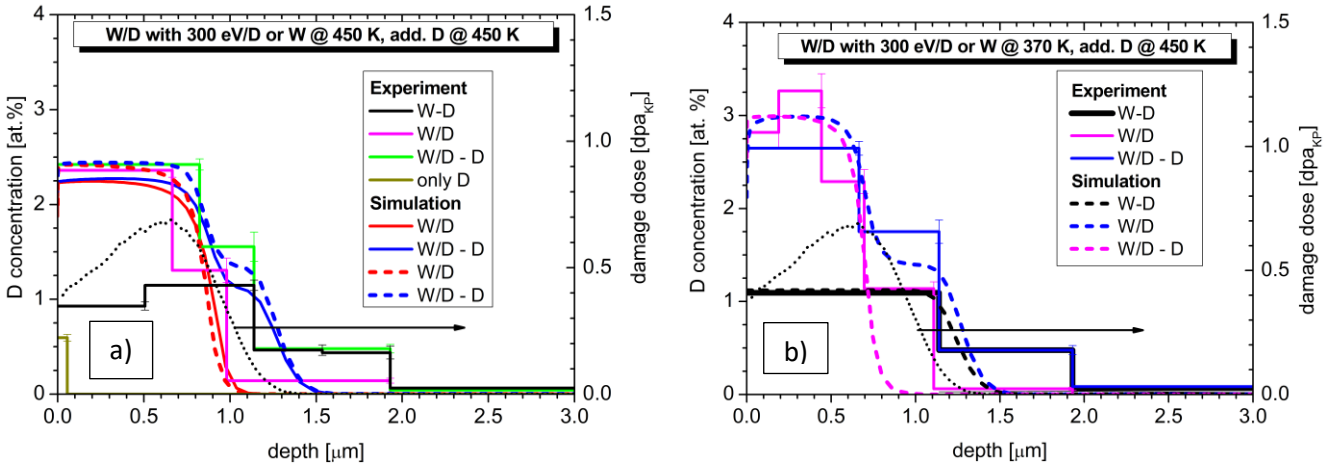

Figure 2: a) Measured and simulated D depth profiles for the simultaneous W/D ion exposure at 450 K for 8 hours and after the additional D ion exposure (W/D-D) also at 450 K. The solid lines (blue and red lines) are MHIMS-R modelling results with parameters determined in [10] *and the dashed lines are new fits by MHIMS-R with one additional fill-level for defect 1. For comparison we also show D depth profiles from a sequential experiment (black line) and a only D exposed, both from* [6]*. b) Measured and simulated D depth profiles after the sequential and simultaneous W ion irradiation at 370 K for 8 hours with additional D ion exposure at 450 K. The solid lines are measured data, the dashed lines are MHIMS-R simulation results. The black dotted line shows an SRIM calculation of the damage depth profile with damage dose values on the right Y scale.*

the created defects by D. This experiment is denoted as "W- D". The W ion irradiation took place for four or eight hours.

The W ion fluence was $(1.0\pm0.15)\times10^{18}$ W/m^2 for four hours and $(2.0\pm0.2)\times10^{18}$ W/m^2 for eight hours irradiation time on the irradiated 5x5 mm^2 square irradiation spot. The displacement damage profile as calculated by SRIM [14] is peak shaped and extends down to about 1.3 μm, shown in figure 2. With the two W fluences we create a damage dose of 0.35 dpa or 0.7 dpa, respectively, at the peak maximum, using Quick calculation option with 90 eV displacement damage energy [15] and evaluating the "vacancy.txt" output.

To quantify the results of the W ion irradiations and D ion exposures we measured the D depth profiles after each step. For this purpose nuclear reaction analysis (NRA) was used utilizing the d(^{3}He, p)^{4}He nuclear reaction. For the NRA analysis a ^{3}He ion beam was used with a size of 2 mm in diameter. The energetic protons were detected using the NRA detector at an angle of 160 degrees. Details of the detection system are presented in detail in [6, 16].

At the end of the exposure and NRA analysis thermal desorption spectroscopy (TDS) was performed in the TESS device at Max Planck Institute for Plasma Physics (IPP), Garching. Samples were heated by a linear ramp of 3 K/min up to a maximum temperature of 1010 K and the desorbed gas was measured by a Pfeiffer DMM 422 quadrupole mass spectrometer. We recorded the following mass channels: m/z=1, 2, 3, 4, 12, 14, 16, 17, 18, 19, 20, 28, 32, 40 and 44. Background contributions were determined in a preceding and a subsequent temperature ramp without the sample or with an outgassed sample in the heating zone, respectively.

3. Simulation

In order to interpret the D depth profiles and D desorption spectra we have used the macroscopic rate equation code MHIMS-R [9, 8, 10, 17]. This code simulates the D and W irradiation, creation of defects and diffusion and trapping of D in the material. For defect creation it takes the depth distribution of primary displacement damage creation by W ions as calculated by SRIM up to 0.2 dpa. Above a damage level of 0.2 dpa defect saturation is taken into account. The interaction between defects and hydrogen isotopes (HI) is based upon a fill-level dependent picture [18, 19, 17], where each defect type is attributed to one defect concentration and can trap several HI at the same time. The number of trapped HI in the defect determines their fill-level and to each fill-level a de-trapping energy is associated. This is in contrast to the classical HI-defect interaction picture where each defect can trap only one HI with a fixed de-trapping energy and concentration. More details about the code description can be found in [9, 17]. In the used code we have also recently incorporated a model which enabled us to simulate the increased D retention due to the presence of D during the defect creation [10, 20]. Higher final HI retention as compared to the experiment where no HI is present during the creation of displacement damage was interpreted as defects being stabilized by the presence of HI. The main parameter

incorporated newly in the upgraded equation [10] for defect creation is the parameter α_i, which enables the increase of the defect density beyond the saturation value determined in the experiment without HI presence (so-called H-free tungsten) during damaging and defines the new defect saturation value. The input parameters for the simulation are those given in [10]. If there will be changes in the modelling input parameters they will be given explicitly in the results section.

4. Experimental and modelling results

4.1 Simultaneous experiment - Longer W/D irradiation time.

Based on the simulation results in the previous paper [10], we have speculated that displacement damage saturation had not yet occurred in the entire damage depth for the four hour irradiation time for the simultaneous W/D experiment at 450 K. We have used the derived simulation parameters to extrapolate the experimental results to larger irradiation times. To test this model prediction, we have repeated the 450 K W/D - D irradiation sequence but this time with a longer W/D exposure time. By doubling the W/D irradiation time from four to eight hours an irradiating W fluence of 2×10^{18} W/m^2 was achieved. For hydrogen-free tungsten D retention starts to saturate beyond a damage dose of 0.1-0.2 dpa [21, 22]. Saturation of defects at this dose was recently also proven by modelling [23, 24]. As derived in [10] we assumed that this also holds for our experiment. The D ion flux was determined to be approximately $(4\pm1)\times10^{18}$ D/m^{2}s while the energy of the D ions was 300 eV/D. After the simultaneous W/D irradiation at 450 K, the sample was re-exposed to the same D ion beam for additional 20 hours to populate all of the created defects. This re-exposure was shorter than the one used in the original experiment (39 hours), because the modelling of the original experiment predicted that such a long D re-exposure was not necessary to populate all of the defects. After the simultaneous W/D irradiation and after the D re-exposure the D depth profile was measured using NRA. Both measured D depth profiles after W/D (magenta line) and after W/D - D (green line) are shown in figure 2a. The SRIM-calculated damaged depth profile is shown as dotted line in the figure. For comparison we also show D depth profiles for the W-D sequential experiment and 300 eV/D D ions only for 39 hours from [6]. For the latter the retention in the bulk is 4×10^{-4} at.% and a small amount of D at the surface of 2×10^{19} D m^{-2}. One can see that after eight hours of exposure D managed to penetrate down to 1 µm what is also approximately the maximum depth of damage crated by the W irradiation. With the additional D ion exposure for 20 h D penetrated a little bit deeper, to populate defects but the maximum D concentration was within error bars the same as for the simultaneous W/D only case. This shows that D stabilized defects throughout the W damage creation depth already in this first experimental step. Please be aware that the D concentration for a sequential W-D experiment at 450 K would be only 1 at.% as measured in ref. [6].

In addition to the above experiments we conducted a sequential W-D and simultaneous W/D - D exposure at lower temperature to study the increased amount even at lower temperatures. Here the W irradiation with or without D ions took place at 370 K but the additional D ion exposure afterwards took place at 450 K for 38 hours in the sequential case and for 28 hours in the simultaneous case. We made the additional D exposure at 450 K to be able to compare directly with the previous results. The D depth profile for the simultaneous and sequential experiment are shown in figure 2b. The SRIM-calculated damage depth profile is again shown as dotted line for comparison. The sequential W-D irradiation resulted in a homogeneous D concentration of 1.1 at.% down to 1.15 µm and then it starts to decrease. This means that we have populated all defects by D throughout the damaged zone and also that the damage dose is above saturation for D in that area. The D concentration is 10 % higher than for the sequential case at 450 K. For the simultaneous experiment one observes a peaked D depth profile with maximum D concentration of 3.3 at.% after the first step W/D at 370 K. The D concentration is higher than for the sequential case throughout the whole damaged region. The D concentration at 370 K after W/D is higher compared to 450 K case, being 2.36 at.%. After the additional D ion exposure at 450 K the maximum D concentration reduces to 2.65 at.% being homogeneous down to 0.7 µm and then decreases step wise to the end of the damaged zone. One can see that the prominent stabilization of defects took place down to 0.7 µm where we see 2.4 times higher D concentration compared to the sequential case. D concentration from 0.7 µm to 1.1 µm is 1.6 times higher compared to the sequential data. Beyond this depth the D depth profiles coincide. When comparing the 370 K case to the 450 K case shown in figure 2a, the D concentration for the 450 K case is lower being 2.4 at.%.

We have also performed TDS analysis on the above described samples. In figure 3 we show the spectrum of the sequential experiment at 370 K and the spectra of the simultaneous experiments performed at 450 K and 370 K for 8 hours and then additional D ion exposure at 450 K. All spectra have two desorption peaks one at about 600 K and the second one at 750 K. The D desorption spectrum for the sequential experiment at 370 K is more than a factor of two lower compared to both simultaneous cases. Also total D amount show almost a factor of two difference, obtaining 8.4×10^{20} D/m^{2}s for the sequential case at 370 K and 17.6×10^{20} D/m^{2}s and 15.5×10^{20} D/m^{2}s for the simultaneous cases at 370 K and 450 K, respectively. From the surface microscopy and the fact that there are no spikes observed in the D desorption spectra in all cases means that no blisters on the surface were created. This means that the increased D retention is due to defect stabilization by D being present during the W irradiation. When we compare the D desorption spectra for the two simultaneous cases we see higher D

desorption for 370 K case as compared to the 450 K experiment. This goes in line with the NRA results when comparing the maximum D concentrations (figure 2).

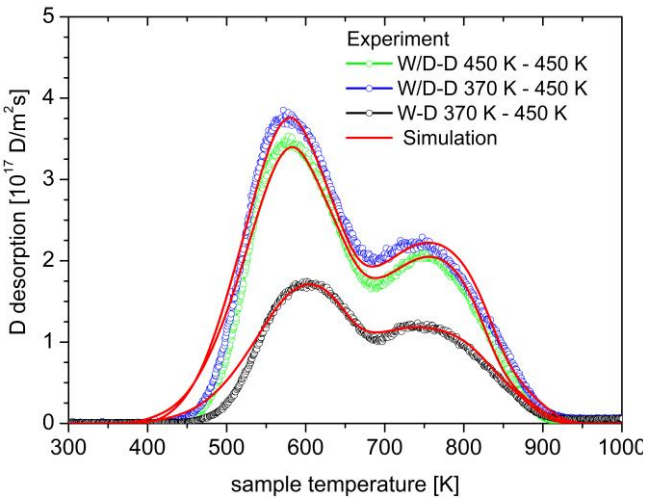

Figure 3: D desorption spectra for the sequential and simultaneous experiments at 370 K and 450 K. The empty circles are experiment and full lines are fit obtained by MHIMS-R. The oven ramp rate was 3K/min.

In figure 2a and 2b we also show the simulation results for D depth profiles calculated with the MHIMS-R code. We will first start to discuss figure 2a and the simultaneous case at 450 K. Using the same input parameters as those determined in [10] (solid lines) we obtain rather good agreement with the experimental profiles. However the D concentration is a bit lower compared to the experiment. Using those parameters also for the simulation of the D desorption spectrum, not shown, it turned out that both peaks are underestimated and the low temperature peak is too narrow. Using similar de-trapping energies and the same defect concentrations but adding a third fill-level for defect 1 and slightly different stabilization parameters we got very good agreement between the experiment and simulation. They agree with the experiment very well, when comparing D desorption spectra, the maximum D concentration and the D penetration depth after each step.

The obtained parameters for the simultaneous experiment at 450 K are:

n_1=0.24 at.% (3 fill-levels, $E_{1,j}$=1.45 eV, 1.32 eV, 1.25 eV), α_1=0.51

n_2=0.29 at.% (2 fill-levels, $E_{2,j}$=1.83 eV, 1.68 eV), α_2=0.375

n_3=0.05 at.% (1 fill-levels, $E_{3,j}$=2.09 eV), α_3=0.08.

Here n_i is the defect concentration, $E_{i,j}$ are the fill-level energies (also called de-trapping energies) and α_i is the stabilization parameter. Comparing the α_i as determined in the previous experiment [10] the α_1 was reduced from 0.66 to 0.51 and α_2 increased from 0.29 to 0.375 and α_3 was increased from 0 to 0.08. We have kept the defect concentrations the same as in [10].

We have fitted also the sequential and the simultaneous experiments at 370 K. We have first fitted the sequential case with which we got the defect concentrations n_i and fill-level energies $E_{i,j}$. By fitting the simultaneous case we determined then the stabilization parameter for each defect. In order to fit those spectra for the experiments at 370 K, we used the following parameters:

n_1=0.29 at.% (3 fill-levels, $E_{1,j}$=1.44 eV, 1.32 eV, 1.25), α_1=0.48

n_2=0.24 at.% (2 fill-levels, $E_{2,j}$=1.85 eV, 1.68 eV), α_2=0.63

n_3=0.06 at.% (1 fill-levels, $E_{3,j}$=2.09 eV), α_3=0.08.

At this point we need to stress that for the sequential case only two fill-levels were needed to fit the D desorption spectrum but for the simultaneous case three fill-levels were needed as was the case for the simultaneous 450 K. Only two had to be assumed and the third one needed to be removed for the sequential case to get a reasonable fit. The simulation also does not reproduce the decrease in D concentration after additional loading at 450 K in the simultaneous case. The reason for this is not clear and would need further research in this direction in the future. We would also like to stress that the D depth profiles and D desorption spectra are not normalized in any way to compare with the MHIMS-R calculation. We have only divided the D desorption flux (D/s) by the area irradiated with the W beam of S=0.28 cm^2. The de-trapping energies for the 450 K case are almost the same as for the case of 370 K case. However, the defect concentrations, as determined from the sequential experiment, for the first and the second defect type are different. The defect concentration n_1 is higher and n_2 is lower for the 370 K case as compared to 450 K case.

4.2 Simultaneous experiment – higher D ion energy.

In addition to longer exposure times and lower exposure temperature we exposed samples at higher D ion energy of 1000 eV/D. By using two different energies of D ions, the implantation depth of the D ions is varied. This in turn affects the mobile concentration of D [8]. The higher the energy of the D ions, the higher their solute concentration is. Solute concentration of D influences the occupation states of the defects. We presume that a higher solute concentration results in occupation of higher fill-levels compared to a lower solute concentration. In the case of 1000 eV/D the flux was measured by a Faraday cup [12] and by the current measured on the sample surface which was 1.5-times higher as compared to 300 eV/D. In this case due to the higher acceleration voltage the ion beam is more peaked which increases the D ion flux to the sample by a factor of two. Therefore the maximum D ion flux was determined to be in the $(8\pm2)\times10^{18}$ D/m^2s range. We performed a simultaneous W/D exposure at 450 K for four

hours. After this D re-exposure was performed again with 1000 eV/D ion energy at 450 K for 5 h, to decorate the created defects. The measured D depth profiles are shown in figure 4. Unfortunately, we do not have the D depth profile for the 1000 eV/D case but we believe that due to low ion flux the D depth profile beyond implantation zone would not look substantially different from the one obtained by 300 eV/D. One can see that due to the higher flux and implantation depth, D managed to penetrate through the whole damaged zone in the first step of simultaneous W/D irradiation. This was not the case for the 300 eV/D case where D ions in the four hours penetrated approximately half of the damage zone [6]. After the additional D exposure, the D depth profile stayed more or less the same as after the first step. Compared with the measured D concentration of 2.4 at.% for the 300 eV/D case shown in figure 2a, D concentration increased up to 3.1 at.%. for the 1000 eV/D case. This indicates that D ion energy, flux or solute influences the population of defects by D during the creation of damage and consequently also the maximum D concentration.

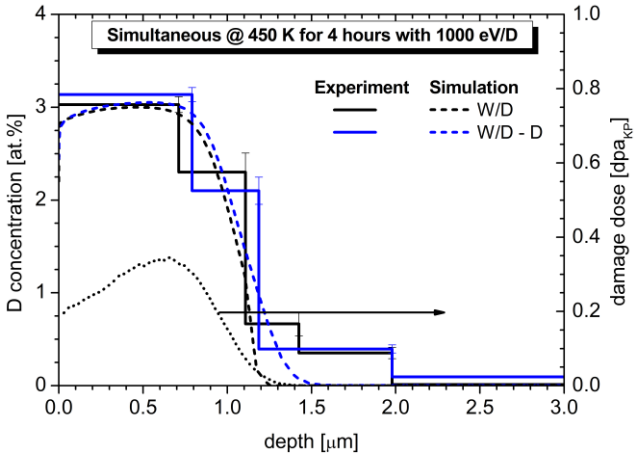

Figure 4: The D depth profiles obtained after the simultaneous experiment at 450 K with D ion energy of 1 keV. The solid lines show the measured D depth profiles and the dashed lines the simulation by MHIMS-R. The black dotted line shows an SRIM calculation of the damage depth profile with damage dose values on the right Y scale.

The TDS spectra are shown for the 1000 eV/D ions at 450 K for the simultaneous W/D - D case in figure 5. For comparison we show also the TDS spectra obtained for the 300 eV/D 8h simultaneous experiment, shown in figure 3. We obtain two desorption peaks as in previous cases but here the low temperature peak is higher and wider in the 1000 eV/D ion energy case as compared to 300 eV/D experiment. The high energy peak stays rather similar. This could indicate that the defect responsible for the low temperature peak has additional fill-levels which are filled with higher D ion energy and D ion flux. We do not see this effect in the case of defects responsible for the high temperature peak that just increases in density due to the defect stabilization but the fill-levels are obviously filled in both D ion exposure case in the same way. If one assumes that the defect 2 is vacancy clusters then according to [25] they have also more fill levels and could take up a lot of additional D. From these experimental data we cannot prove or disprove this.

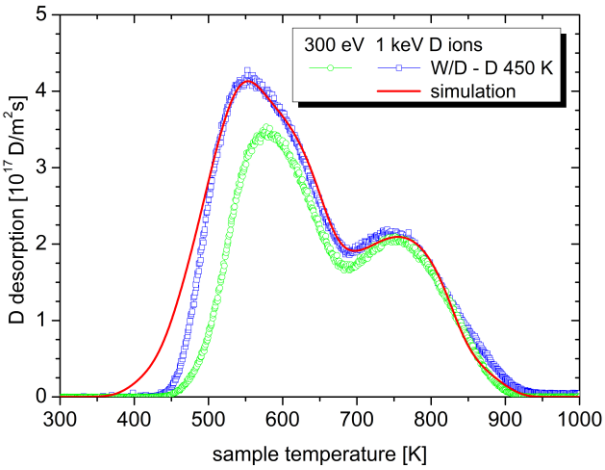

Figure 5: D desorption spectra obtained for simultaneous 1000 eV/D W/D – D ion exposures at 450 K. For comparison we also show the D desorption spectra obtained with 300 eV/D also at 450 K. The oven ramp rate was 3K/min.

Also for this case we have performed the MHIMS-R calculation, using the same input parameters as those used for the 300 eV/D simultaneous case, given above. We have obtained good agreement with the D depth profiles and D desorption spectra only when one additional fill-level was added (now four in total) and the stabilization parameter for defect 1 was just slightly increased from 0.51 to 0.55. When simulating the 300 eV/D case shown in figure 2a and 3 with four fill levels we could not reproduce the D desorption spectra since the fourth fill level was also filled in the simulation ending up with higher D concentration and wider D desorption spectrum. This is not observed in the experiment. The reason for this discrepancy is not clear at the moment but is could be due to not simulating properly the cooling down phase and the phase between end of exposure and TDS. It could also be that the surface boundary conditions affect the filling of the different fill levels at different conditions. This issue would need further investigation experimentally and modelling in the future. The optimal fitting parameters for the 1000 eV/D case at 450 K are:

n_1=0.24 at.% (4 fill-levels, $E_{1,j}$=1.45 eV, 1.34 eV, 1.23 eV, 1.16 eV), α_1=0.55

n_2=0.29 at.% (2 fill-levels, $E_{2,j}$=1.83 eV, 1.68 eV), α_2=0.375

n_3=0.05 at.% (1 fill-levels, $E_{3,j}$=2.09 eV), α_3=0.08.
Some de-trapping energies for defect 1 were just slightly changed (~ 0.02 eV) as compared to the parameters given above also for 450 K simultaneous case which steams from the accuracy of the temperature measurement on the sample during TDS as discussed in [20]. The fact that defect 1 has more fill-levels than two as determined in [10] was observed already when the TDS spectra and D depth profiles for the experiments described in [26, 20] were fitted. In those cases W samples were irradiated by 20 MeV W ions at 300 K and then exposed to low temperature plasma with almost one order of magnitude higher flux and at a temperature of 370 K. For those experiments five fill-levels were needed for defect 1 with the following fill-level energies (1.46±0.03, 1.34±0.03, 1.25±0.02, 1.16±0.02, 1.08±0.03) eV. The defect 2 that is responsible for majority of the high temperature peak has 2 fill-levels in all cases. We can observe that within error bars we used the same energies for individual fill-levels.

In addition to the 450 K exposures we have performed simultaneous and sequential exposures with higher D ion energy also at an irradiation temperature of 800 K. The additional D ion re-exposure was performed at 450 K to populate the created defects. These exposures were also done with an energy of 1000 eV/D. We have performed this experiment since in the first study with 300 eV D ions the stabilization of defects was minor at 800 K [6]. The measured D depth profiles after each step are shown in figure 6. Additionally, we compare the present results with those obtained with 300 eV/D energy from [6].

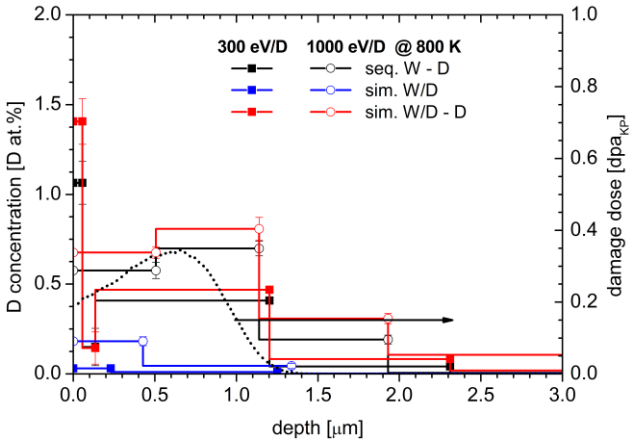

Figure 6: The D depth profiles obtained after the simultaneous and sequential experiment at 800 K with D ion energy of 1 keV with the additional exposure at 450 K. For comparison we also show experiments made with 300 eV/D ions from [6]. *The black dotted line shows an SRIM calculation of the damage depth profile with damage dose values on the right Y scale.*

In the first step of simultaneous W/D at 800 K we can observe that the D concentration is higher for the 1000 eV/D case as compared to 300 eV/D case by a factor of about 5 down to depth of 1.3 μm. The additional D re-exposure results in a D concentration of 0.68 at % and 0.8 at.%, in steps down to 1.3 μm. For the sequential experiment the D concentration is slightly lower with 0.58 at. % and 0.7 at. %. The difference of 15 % between the simultaneous experiment and sequential experiment is surprisingly the same as in the case of the 300 eV/D case. This indicates that the higher D ion flux and energy did not result in higher stabilization of defects due to the D presence as was the case at 450 K. This could mean that the D concentration that we had during the first step of simultaneous exposure is not sufficient to cause a substantial stabilization of defects. Interestingly, the present sequential experiment at 800 K gives a higher D concentration as compared to data from [6] being 0.4 at.%. The TDS spectra, not shown, show increase in both TDS peaks. This indicates that both defects 1 and 2 have more filling levels that can be filled with higher flux. Comparing the 800 K experiment to 450 K experiment at the same energy one observes a substantial drop in D concentration during W/D which is due to efficient D de-trapping at high temperatures. After the additional loading at 450 K we obtain lower D concentration since the defects are annihilated at higher temperatures and the stabilization due to D presence is smaller due to lower D concentration in the first step.

5. Discussion and conclusions

In this work we studied how parameters like D ion flux, D ion energy, W/D irradiation temperature and time influence the effect of defect stabilization due to HI presence. It was clearly shown that higher D ion flux and energy fills more fill-levels for defect 1 and increases the final D concentration in the damaged region as shown for the 450 K case at different exposure conditions. In addition lower W irradiation temperature of 370 K results also in higher final D concentration for the same D ion energy because the D concentration in the sequential case, the hydrogen-free case, is slightly higher and due to higher D concentration during W/D which leads to higher defect stabilization. The D concentration is still lower than for the 1000 eV/D case at 450 K where even higher D concentration during the W/D was measured and results in even higher stabilisation of defects. From simulation we see that the difference is due to filling of the fourth fill level in the 1000 eV/D case. A summary of final maximum D concentrations is shown in figure 7. There the maximum D concentrations obtained in this study were added to the ones obtained in [6] where a series of simultaneous and sequential experiments were performed at different temperatures with 300 eV/D also in INSIBA setup. Additionally, we show for comparison also the data from [20, 27] where 20 MeV W irradiations at 300 K and D plasma exposures at 370 K were performed several times. Namely, after W-D sequence additional W-D sequences were preformed, named double and

triple W/D. In the second and third step the D was present during the W irradiation at 300 K and for this reason it needs to be compared to the simultaneous data. After each W irradiation samples were exposed to D plasma at 370 K which resulted after each step in further increase of D concentration. With the help of simulation it was shown that proceeding with W damaging and D loading steps one would end up in saturation D concentration of 4.2 at.% [20]. We can conclude that the additional fill-levels available for defect 1 enable to increase the D concentration for the different cases studied here but we did not exceed the D saturation concentration of 4.2 at.% as was determined for a series of W-D irradiation steps [20]. With this one can say that for DEMO where orders of magnitude higher fluxes are expected [1, 2, 28] the saturation will be set when all fill-levels are filled with the stabilization parameters similar to the ones obtained in this study. These effects however will be only very efficient at lower temperatures. At higher temperatures the de-trapping of HI from the defects prevails meaning less HI-filled defects and lower stabilization of defects. Based on the results of the simultaneous and sequential experiment at 800 K it also seems that there could exist a low level of HI concentration where stabilization has no longer a significant effect on the defect stabilization due to the presence of HI.

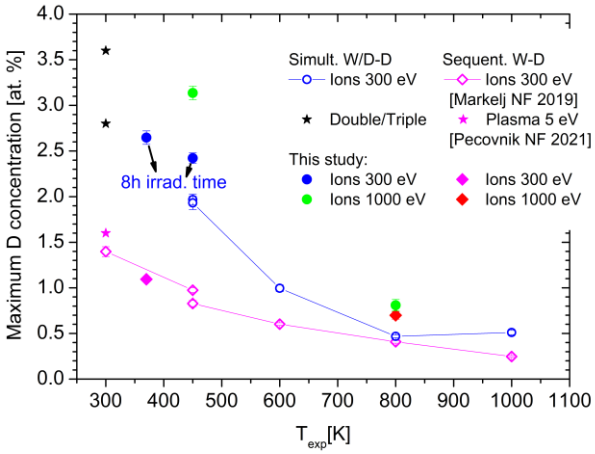

Figure 7: Maximum D concentrations as obtained from the D depth profiles in the present study at different experimental conditions performing simultaneous and sequential exposures at different W irradiation temperatures. In all cases the additional D ion exposures were made at 450 K. The data are compared to previous study in the same experimental set up, empty signs [6]. *We show also the data for series of sequential W-D exposures using 20 MeV W ions at 300 K and 5 eV plasma at 370 K* [27, 20], *marked as stars.*

Acknowledgements

Authors would like to acknowledge to Etienne Hodille for fruitful discussion with regard to modelling. This work has been carried out within the framework of the EUROfusion Consortium and has received funding from the Euratom research and training programme 2014-2018 and 2019-2020 under grant agreement No 633053. The views and opinions expressed herein do not necessarily reflect those of the European Commission. The authors acknowledge the support from the Slovenian Research Agency (research core funding No. P2-0405).

References

[1] G. A. Spagnuolo et al., "Integration issues on tritium management of the European DEMO Breeding Blanket and ancillary systems," *Fusion Engineering and Design,* vol. 171, p. 112573, 2021.

[2] R. Arredondo, K. Schmid, F. Subba and G. A. Spagnuolo, "Preliminary estimates of tritium permeation and retention in the first wall of DEMO due to ion bombardment," *Nuclear Materials and Energy,* vol. 28, p. 101039, 2021.

[3] M. Rieth and e. al., "Recent progress in research on tungsten materials for nuclear fusion applications in Europe," *J. Nucl. Mater.,* vol. 432, p. 482–500, 2013.

[4] T. Tanabe, "Review of hydrogen retention in tungsten," *Phys. Scr.,* vol. T159, p. 014044, 2014.

[5] S. Markelj, T. Schwarz_Selinger, A. Zaloznik, M. Kelemen, P. Vavpetic, P. Pelicon, E. Hodille and C. Grisolia, "Deuterium retention in tungsten simultaneously damaged by high energy W ions and loaded by D atoms," *Nucl. Mater. Energ.,* vol. 12, pp. 169-174, 2017.

[6] S. Markelj et al., "Displacement damage stabilization by hydrogen presence under simultaneous W ion damage and D ion exposure," *Nucl. Fusion 59,* p. 086050, 2019.

[7] A. Zaloznik, S. Markelj, T. Schwarz-Selinger and K. Schmid, "Deuterium atom loading of self-damaged tungsten at different sample temperatures," *J. Nucl. Mater.,* vol. 496, pp. 1-8, 2017.

[8] E. Hodille, S. Markelj, T. Schwarz-Selinger, A. Zaloznik, M. Pecovnik, M. Kelemen and C. Grisolia, "Stabilization of defects by the presence of hydrogen in tungsten: simultaneous W-ion damaging and D-atom exposure," *Nucl. Fusion,* vol. 59, p. 016011, 2019.

[9] E. A. Hodille, X. Bonnin, R. Bisson, T. Angot, C. S. Becquart, J.-M. Layet and C. Grisolia, "Macroscopic rate equation modeling of trapping/detrapping of hydrogen isotopes in tungsten materials," *J. Nucl. Mater. ,* vol. 467, pp. 424-431, 2015.

[10] M. Pečovnik, S. Markelj, E. Hodille, T. Schwarz-Selinger and C. Grisolia, "New rate equation model to describe displacement damage stabilization by hydrogen atoms in tungsten," *Nuclear Fusion,* vol. 60, p. 036024, 2020.

[11] D. Kato, H. Iwakiri , Y. Watanabe, K. Morishita and T. Muroga, "Super-saturated hydrogen effects on radiation damages in tungsten under the high-flux divertor plasma irradiation," *Nucl. Fusion,* vol. 55, p. 083019, 2015.

[12] M. Kelemen et al., "Influence of surface roughness on the sputter yield of Mo under keV D ion irradiation," *J. Nucl. Mater.,* vol. under review, 2021.

[13] T. Schwarz-Selinger, A. Von Keudell and W. Jacob, "Novel method for absolute quantification of the flux and angular distribution of a radical source for atomic hydrogen," *Journal of Vacuum Science & Technology A: Vacuum, Surfaces, and Films,* vol. 18, p. 995–1001, 2000.

[14] J. Ziegler, "www.srim.org.," [Online].

[15] ASTM Int'l E521-16, "Standard practice for neutron radiation damage simulation by charge-particle irradiation," in *Annual Book of ASTM Standards vol 12.02*, Philadelphia, PA, American Society for Testing and Materials, 2016, p. p 8.

[16] S. Markelj et al., "Deuterium transport and retention in the bulk of tungsten containing helium: the effect of helium concentration and microstructure," *Nucl. Fusion,* vol. 60, p. 106029, 2020.

[17] E. A. Hodille et al., "Study of hydrogen isotopes behavior in tungsten by a multi trapping macroscopic rate equation model," *Phys. Scr.,* vol. T167, p. 014011, 2016.

[18] K. Heinola, T. Ahlgren, K. Nordlund and J. Keinonen, "Hydrogen interaction with point defects in tungsten," *Phys. Rev. B ,* vol. 82, p. 094102, 2010.

[19] N. Fernandez, Y. Ferro and D. Kato, "Hydrogen diffusion and vacancies formation in tungsten: Density Functional Theory calculations and statistical models," *Acta Mater. ,* vol. 94, pp. 307-318, 2015.

[20] M. Pečovnik, T. Schwarz-Selinger and S. Markelj, "Experiments and modelling of multiple sequential MeV ion irradiations and deuterium exposures in tungsten," *Journal of Nuclear Materials,* vol. 550, p. 152947, 2021.

[21] V. Alimov, Y. Hatano, B. Tyburska-Püschel, K. Sugiyama, I. Takagi, Y. Furuta, J. Dorner, M. Fußeder, K. Isobe, T. Yamanishi and M. Matsuyama, "Deuterium retention in tungsten damaged with W ions to various damage levels," *J. Nucl. Mater.,* vol. 441, p. 280–285, 2013.

[22] O. V. Ogorodnikova and V. Gann, "Simulation of neutron-induced damage in tungsten by irradiation with energetic self-ions," *J. Nucl. Mater.,* vol. 460, p. 60, 2015.

[23] P. M. Derlet and D. S. L., "Microscopic structure of a heavily irradiated material," *Phys. Rev. Materials,* vol. 4, p. 023605, 2020.

[24] D. R. Mason et al., "Parameter-free quantitative simulation of high-dose microstructure and hydrogen retention in ion-irradiated tungsten," *Phys. Rev. Materials,* vol. 5, p. 095403, 2021.

[25] J. Hou, X.-S. Kong, X. Wu, J. Song and C. S. Liu, "Predictive model of hydrogen trapping and bubbling in nanovoids in bcc metals," *Nat. Mater. ,* vol. 18, p. 833–839, 2019.

[26] M. Pecovnik, S. Markelj, M. Kelemen and T. Schwarz-Selinger, "Effect of D on the evolution of radiation damage in W during high temperature annealing," *Nuclear Fusion,* vol. 60, p. 106028, 2020.

[27] Schwarz-Selinger, T., Bauer, J., Elgeti, S. and S. Markelj, "Influence of the presence of deuterium on displacement damage in tungsten," *Nucl. Materials and Energy,* vol. 17, p. 228–234, 2018.

[28] G. R. Tynan et al., "Deuterium retention and thermal conductivity in ion-beam displacement-damaged tungsten," *Nuclear Materials and Energy,* vol. 12, p. 164–168, 2017.